

# Evaluation of High Ni-Cr-Mo Alloys for the Construction of Sulfur Dioxide Scrubber Plants

N. Rajendran and S. Rajeswari

Corrosion in wet lime/limestone systems used for flue gas desulfurization in thermal power plants is of great concern. The frequent variations in acidity and in chloride and fluoride ion concentrations experienced by such systems pose a serious threat to the materials of construction. Currently used materials mostly type 316L stainless steel often fail to meet their life expectancy. The present study evaluates the performance of advanced Ni-Cr-Mo alloys 59 and C-276 in a simulated sulfur dioxide scrubber environment. Accelerated tests showed that high Ni-Cr-Mo alloys have little tendency to leach metal ions such as chromium, nickel, and molybdenum at different impressed potentials. Scanning electron microscopy was used to examine the morphology of pitting attack.

## Keywords

accelerated leaching, Alloy 59, Alloy C-276, flue gas desulfurization, Ni-Cr-Mo alloys, pitting corrosion

## 1. Introduction

AIR pollution management is the major economic and environmental challenge of this decade. Technologically advanced countries continue to rely heavily on coal for their energy needs, and coal-fired power stations are the major contributors of power in developing countries. The vital problem with the increased use of coal in thermal power plants is the threat posed by sulfur dioxide emissions. To control this dangerous atmospheric pollutant, various methods have been adopted and are in various stages of development. These include removing sulfur prior to combustion and scrubbing the flue gas generated by combustion.

The latter method is known as tail-end removal or flue gas desulfurization (FGD) (Ref 1). The FGD scrubbers (also called SO<sub>2</sub> scrubbers) have found widespread use in thermal power plants, smelters, incinerators, and various refining operations (Ref 2-7). Several studies (Ref 8, 9) have shown that the capital cost incurred in installing an FGD system amounts to almost 25% of the total installation cost for the entire thermal power plant. It is obvious that measures must be taken to prevent degradation of FGD systems by corrosion and other related phenomena.

However, the materials of construction used for FGD systems (typically, type 316L stainless steel) often fail due to localized corrosion, such as pitting and crevice corrosion attack. Such attack can be induced by the aggressiveness of the environment created by the presence of chloride and fluoride ions, by acidity (H<sup>+</sup> ion), and by the temperature encountered during SO<sub>2</sub> scrubbing (Ref 1, 5, 10, 11). Improving the corrosion performance of current construction materials can be achieved through alloying with suitable elements.

The present study investigated the localized corrosion behavior of Alloys 59 and C-276 (a product of VDM Corporation Ltd.) by means of electrochemical methods. The pitting corro-

sion resistance of the alloys at various temperatures was evaluated, as was their performance in accelerated leaching in a simulated SO<sub>2</sub> scrubber system.

## 2. Methods and Materials

### 2.1 Electrode Preparation

The chemical compositions of Alloy 59, Alloy C-276, and type 316L stainless steel are given in Table 1. Sheet materials in the as-received condition were cut into 1 by 1 by 0.3 cm specimens for electrochemical study, which simplified measurement of current density. The specimens, attached with a brass rod for electrical connection, were mounted in an epoxy-base resin such that only one side with a 1 cm<sup>2</sup> surface area was exposed; this formed the working electrode. To avoid the need for severe polishing after resin mounting (which might cause crevices at the metal/resin interface), the specimens were wet ground with SiC papers down to 800 grit, followed by a 5 μm diamond paste. The electrodes were then ultrasonically cleaned in acetone, thoroughly washed in distilled water, and dried using acetone.

### 2.2 Electrochemical Cell Assembly

The electrochemical cell consisted of three compartments with a capacity of 500 mL. Saturated calomel electrode (SCE) was used as the reference electrode, platinum foil as the counter electrode, and the specimen as the working electrode. The electrolyte solution contained chloride, fluoride, and sulfite to simulate the SO<sub>2</sub> scrubber environment, the composition and operating conditions of which are as follows:

Chemical composition	
Chloride ion, ppm	10,000
Fluoride ion, ppm	1,000
Sulfite ion, ppm	2,000
Operating conditions	
pH	5.0
Temperature, °C	52 ± 2

The pH of the electrolyte was adjusted with sulfuric acid. The working electrode was then introduced into the cell, and the potential was allowed to stabilize for 15 min.

N. Rajendran and S. Rajeswari, Department of Analytical Chemistry, University of Madras, Guindy Campus, Madras 600 025, India.

## 2.3 Polarization Study

In the cyclic potentiodynamic polarization study, the potential was increased from rest potential in the noble direction at a rate of 1 mV/s until the breakdown potential ( $E_b$ ) was attained where the alloy entered the passive/transpassive region. The sweep direction was then reversed after reaching an anodic current density of 1 mA/cm<sup>2</sup> until the potential where the reverse scan current density equals the forward scan current density. The potential at which the reverse anodic scan cuts the forward scan is called the pit-protection potential ( $E_p$ ) or pit repassivation potential ( $E_r$ ). The pitting potentials of the alloys were determined at room temperature, at 50 °C, and at 80 °C.

The parameters of interest recorded during the polarization studies included:

- Corrosion potential,  $E_{corr}$
- Pitting potential,  $E_b$
- Pit-protection potential,  $E_p$
- Region safe from corrosion attack,  $\Delta E$

**Table 1** Chemical compositions of the alloys

Alloy	Composition, wt %						
	Ni	Cr	Mo	Fe	W	Mn	C
316L	12.2	17.2	2.4	bal	...	2.0	0.03
59	59	23	16	1	...	0.45	0.01
C-276	57	16	16	5	3.5	0.43	0.01

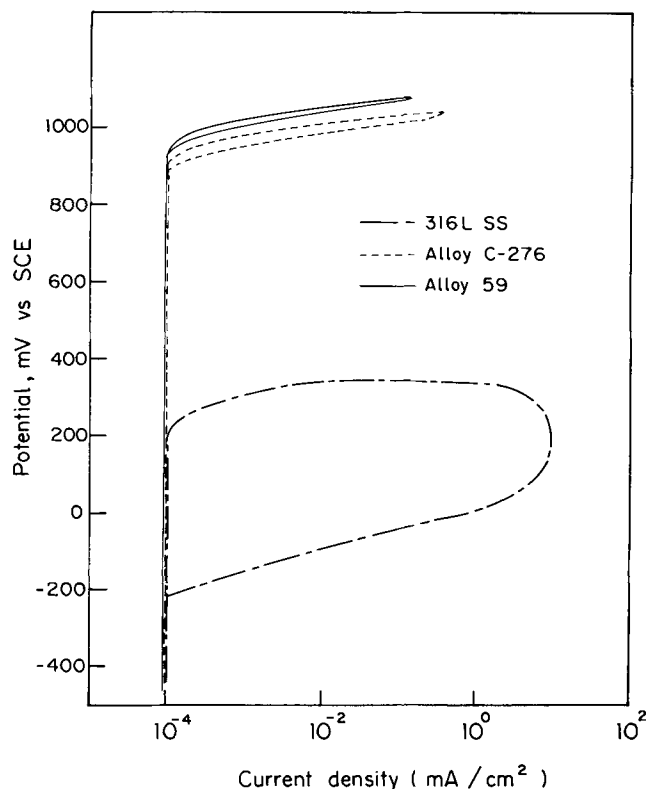


**Fig. 1** Potentiodynamic anodic cyclic polarization curves for type 316L stainless steel, Alloy C-276, and Alloy 59 in the simulated SO<sub>2</sub> scrubber environment

## 2.4 Pit Morphology Studies

A Hitachi scanning electron microscope (SEM) was used to examine pit morphology.

## 2.5 Accelerated Leaching of Nickel, Chromium, and Molybdenum

In the accelerated leaching studies, the working electrodes were immersed in the simulated SO<sub>2</sub> scrubber environment and allowed to stabilize at potentials of +100, 200, 300, 500, and  $E_b$  for 1 h in 100 mL of the test solution. At the end of each experiment, the chemical composition of the test solution was analyzed by inductively coupled plasma atomic emission spectroscopy.

## 3. Results and Discussion

### 3.1 Critical Pitting Potential

Pitting potential was the criterion used to evaluate the pitting corrosion resistance of the materials. The pitting potential of an alloy is directly influenced by the amount of passivating elements present in the alloy as well as in the environment. Figure 1 shows the anodic polarization curves for Alloy 59, Alloy C-276, and type 316L stainless steel. The mean value of critical pitting potential ( $E_b$ ) for the type 316L was 240 mV. The presence of 16% Mo and 59% Ni in Alloy 59 acted to increase the  $E_b$  value to 950 mV, and the presence of 16% Mo, 57% Ni, and 3.8% W in Alloy C-276 increased  $E_b$  to 930 mV. Thus, it is evident that high nickel and molybdenum contents increased the pitting potential in a more noble direction, thereby improving the pitting corrosion resistance of alloys 59 and C-276 in the simulated SO<sub>2</sub> scrubber system.

Several studies have indicated that small additions of molybdenum can improve pitting and passivation characteristics. Sakashita and Sato (Ref 12) have suggested that when cation-selective molybdate ions adsorb onto relatively thick membranes of an anion-selective hydrated iron oxide, they can alter ionic transport through the film by inducing ionic rectification. Streicher (Ref 13) has suggested that the combined addition of chromium and molybdenum to alloys greatly improves their corrosion resistance in acidic chloride solutions, with molybdenum interacting synergistically with chromium. Yang et al. (Ref 14) reported that the presence of molybdenum inhibits the corrosion process through the formation of a molybdenum salt film, which apparently is difficult to break down.

The effect of temperature on pitting potential is shown in Fig. 2. Alloys 59 and C-276 exhibited a higher resistance to pitting attack over a wide range of temperatures, whereas type 316L stainless steel had low corrosion resistance at all temperatures studied. Mitrovic-Scepanovic and Ives (Ref 15) have studied the electrochemical behavior of all the oxides of molybdenum; their results permit one to assume that a mixed oxide phase of type  $(Mo^{4+}, Mo^{6+})_xO_y$  could be present in the films on the higher-molybdenum alloys, due to its much higher thermodynamic stability. Agarwal and Heubner (Ref 16) have noticed that high chromium and molybdenum contents significantly improve corrosion resistance even at higher thermal conditions.

The pit morphology observed with SEM is shown in Fig. 3. The type 316L stainless steel exhibited individually larger and deeper individual pits over the entire surface of the specimen (Fig. 3a), indicating higher susceptibility of the material to pitting attack. The increased amounts of passivating elements such as molybdenum, chromium, and nickel (16, 23, and 59%, respectively) in Alloy 59 (Fig. 3b) resulted in a very low number of pits compared to the reference 316L stainless steel. An almost identical pitting behavior was observed for Alloy C-276 (Fig. 3c).

The SEM study clearly shows that materials with greater corrosion resistance exhibit a lower depth of pitting attack, whereas materials with lesser corrosion resistance reveal a greater depth of pitting attack. This could be due to a low pH within the pits of type 316L, resulting in an aggressive environment and thus accelerating the propagation of pits. On the other hand, in the higher-nickel alloys, resistance to pitting attack can be attributed to the hydrolysis of nickel. The passivation of nickel alloys is by oxide film formation, which involves a reaction such as:



where there is a direct electrochemical reaction between the working electrode and water in the solution.

The hydrolysis of  $\text{Ni}^{2+}$  yields essentially a neutral pH, so that the dissolved nickel ions are unlikely to contribute to acidification of the solution within the pit and crevice. As a result, the aggressiveness of the environment within the pits is reduced.

### 3.2 Pit Protection Behavior

The pit-protection potential ( $E_p$ ) was determined for the three alloys from their polarization curves (Fig. 1). The mean value of  $E_p$  for type 316L increased from -210 to +935 mV with

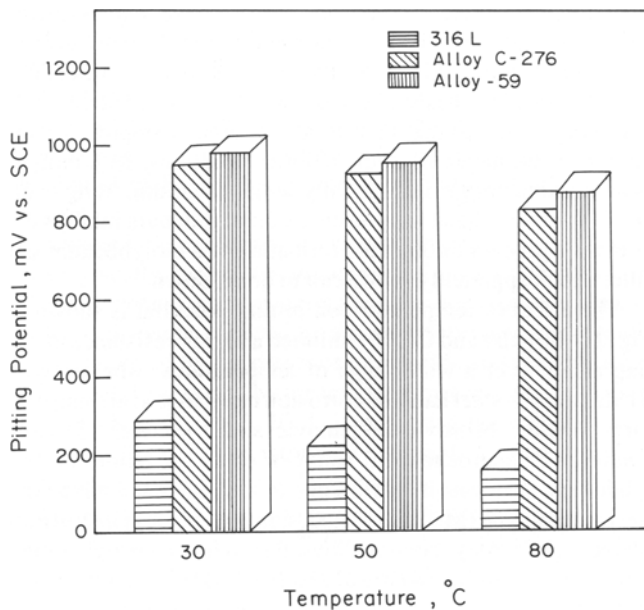
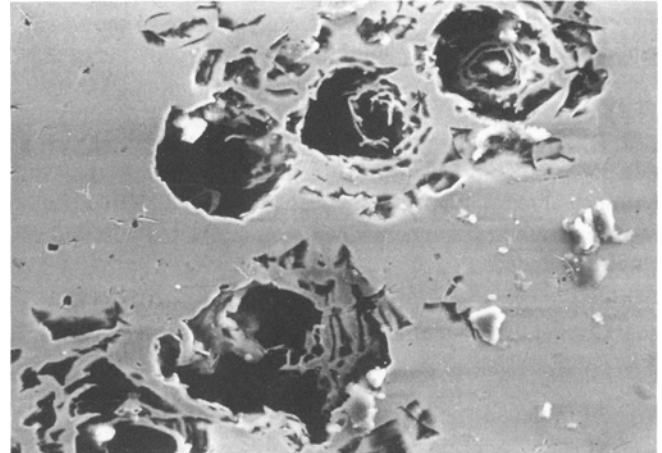
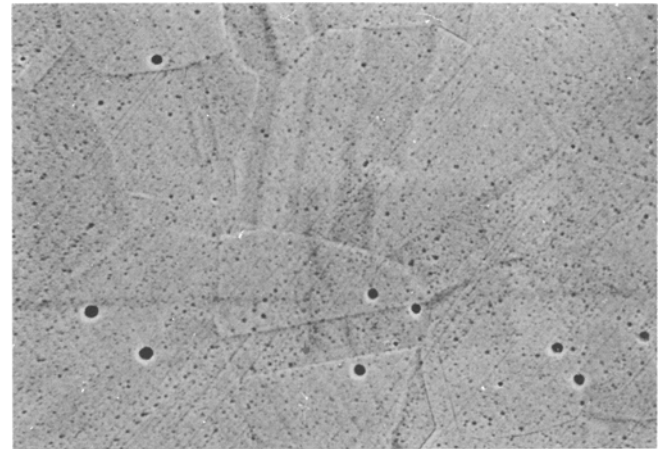


**Fig. 2** Temperature dependence of pitting potential in the simulated  $\text{SO}_2$  scrubber environment

the addition of 16% Mo, 59% Ni, and 23% Cr in Alloy 59; for Alloy C-276,  $E_p$  increased from -210 to +912 mV. Because new pits cannot be initiated above this pit-protection potential, it can be inferred that increased amounts of chromium, nickel,



(a)



(b)



(c)

**Fig. 3** Scanning electron micrographs of pitting morphology after breakdown of the passive film in the simulated  $\text{SO}_2$  scrubber environment. (a) Type 316L. (b) Alloy 59. (c) Alloy C-276

and molybdenum hinder the development of new pits and also slow the kinetics of growing pits.

Several studies (Ref 17-19) have shown that  $\text{MoO}_4^{2-}$  was detected in all passive films formed on molybdenum-bearing alloys in acidic solutions. These  $\text{MoO}_4^{2-}$  anions are responsible for producing a bipolar film consisting of a cation-selective outer layer and an intrinsically anion-selective inner layer. The bipolarity of the duplex film was considered to be largely responsible for the development of an interfacial barrier layer composed mainly of  $\text{Cr}(\text{OH})_3$ , which resists  $\text{Cl}^-$  and  $\text{OH}^-$  ingress. Both factors should provide greater resistance to breakdown of passivity in chloride-containing media. Molybdenum could form  $\text{Mo}^{6+}$  oxide in the passive film, thereby blocking the penetration of  $\text{Cl}^-$  attack, or alternatively could decrease the rate of dissolution by the formation and retention of molybdenum oxyhydroxide of molybdate at active areas (Ref 20).

With regard to repassivation potential, our results confirm that alloys 59 and C-276 are clearly superior to lower Ni-Cr-Mo alloys. The difference between the pit-protection potential and the corrosion potential for a given system is defined as the relative corrosion resistance ( $\Delta E$ ); the respective corrosion potentials for type 316L, Alloy 59, and Alloy C-276 are  $-435$ ,  $-405$ , and  $-414$  mV. The relative corrosion resistance values can be used to rank the alloys (Ref 21, 22). The mean value of  $\Delta E$  for type 316L was 225 mV. Greater nickel, molybdenum, and chromium contents increased the  $\Delta E$  values to 1340 mV in the case of Alloy 59 and to 1326 mV for Alloy C-276. A higher  $\Delta E$  value reflects enhanced resistance to pitting attack.

### 3.3 Accelerated Leaching in Simulated FGD Environment

In the accelerated leaching study, the concentrations of metal ions (namely, nickel, chromium, and molybdenum) present in the test solution after ageing for 1 h were determined; the results are shown in Fig. 4 to 6. Pitting attack of type 316L occurred at +240 mV; consequently, the leaching study was not conducted at +300 and +500 mV. Significant amounts of metal ions were released into the solution, even in the passive region, for type 316L. In contrast, alloys 59 and C-276 showed little tendency for the leaching of metal ions at impressed potentials of +100, +200, +300, and +500 mV.

Normally, the leaching of metal ions from the construction material initially involves the adsorption of aggressive halide ions at discrete sites on a passive metal surface. This process results in a continuous thinning of the passive film until the bare metal surface is reached at the end of the induction period. Kruger (Ref 23) and Hoar and Jacob (Ref 24) suggested the formation of a transitional complex by the adsorption of three or four halide ions on the surface of the passive film around a lattice cation. Once the complex is formed, it will readily remove the cation from the passive film lattice as a soluble species. Thus, thinning of the film occurs at the site where complex is formed, resulting in a stronger anodic field. This field rapidly

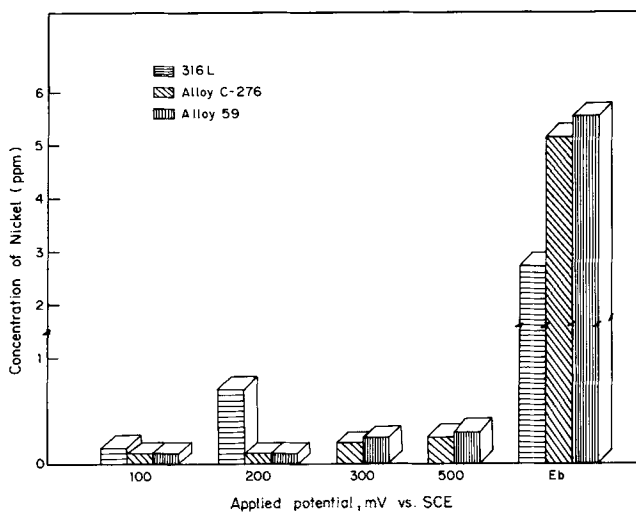


**Fig. 4** Concentration of nickel present in solution after accelerated leaching of type 316L, Alloy C-276, and Alloy 59 at different imposed electrode potentials

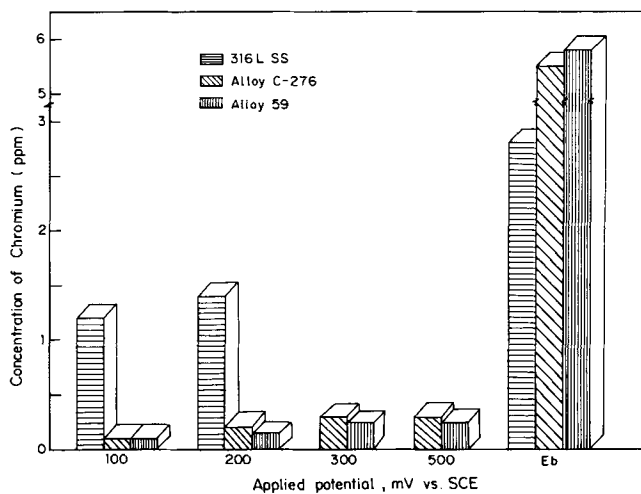


**Fig. 5** Concentration of chromium present in solution after accelerated leaching of type 316L, Alloy C-276, and Alloy 59 at different imposed electrode potentials

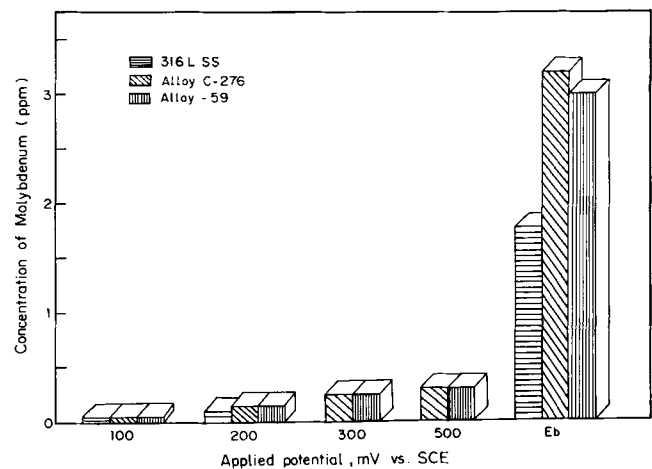


**Fig. 6** Concentration of molybdenum present in solution after accelerated leaching of type 316L, Alloy C-276, and Alloy 59 at different imposed electrode potentials

pulls another cation through the thinned site of the film during the course of its interaction with halide ions. This again results in a soluble complex formation. The traverse of cations of the passive film is thus facilitated until the bare metal is reached.

In the present investigation, alloys 59 and C-276 showed very little tendency to leach metal ions compared to type 316L at impressed potentials of +100, +200, +300, and +500 mV. This can be attributed to the oxide film, which inhibits metal dissolution by forming a physical barrier between the metal and the environment, thus preventing bare metal from contact with solution (Ref 25). At their pitting potential, however, alloys 59 and C-276 showed an enhanced leaching of metal ion concentrations, following this order: type 316L < Alloy C-276 < Alloy 59.

This can be related to the potential at which pitting occurs in these alloys. Molybdenum improves passive film formation; thus, a higher potential is required to initiate pitting of alloys 59 and C-276. Once this potential is reached, however, pits may grow faster, resulting in a greater release of metal ions.

#### 4. Conclusions

Several conclusions can be drawn from the present investigation:

- The critical pitting and pit-protection potentials of alloys 59 and C-276 were more noble than those of type 316L stainless steel. This indicated the beneficial effect of chromium, molybdenum, and nickel in improving corrosion resistance.
- An accelerated leaching study indicated that the release of chromium, nickel, and molybdenum from alloys 59 and C-276 was considerably lower compared to type 316L.
- The pitting resistance of alloys 59 and C-276 in a simulated SO<sub>2</sub> scrubber environment is maintained over a wide temperature range (room temperature, 50 °C, and 80°C).

#### References

1. N. Rajendran, K. Ravichandran, and S. Rajeswari, *Anti-Corros. Methods Mater.*, Vol 42 (No. 1), 1995, p 8
2. R. Roth, *Werkst. Korros.*, Vol 43, 1993, p 275
3. D.B. Anderson, *Corrosion/81*, National Association of Corrosion Engineers, 1981, p 13
4. A.I. Asphahani, A.F. Nicholas, W.L. Silence, and T.H. Mayor, *Werkst. Korros.*, Vol 40 (No. 7), 1989, p 409
5. M.X. Cerney, *Corros. Rev.*, Vol 8 (No. 1/2), 1988, p 60
6. R.R. Skabo, in *Proc. Conf. Solving Corrosion Problems in Air Pollution Control Equipment*, National Association of Corrosion Engineers, 1981, p 2
7. G.D. Jones, P.F. Ellis, D.M. Anlinker, and D.A. Stewart, "Failure Analysis of FGD System Components," presented at 9th Symp. Flue Gas Desulfurization (Cincinnati), 1985
8. M.G. Fontana, *Corrosion Engineering*, 3rd ed., McGraw-Hill, 1987, p 416
9. N. Rajendran, K. Ravichandran, and S. Rajeswari, *Anti-Corros. Methods Mater.*, Vol 42 (No. 2), 1995, p 9
10. C.S. Young, in *Titanium for Energy and Industrial Applications*, D. Eylon, Ed., TMS-AIME, 1981, p 323
11. N. Rajendran, K. Ravichandran, and S. Rajeswari, *Bull. Electrochem.*, Vol 9 (No. 1), 1993, p 4
12. M. Sakashita and N. Sato, in *Passivity of Metals*, R.P. Frankenthal and J. Kevgerh, Ed., Electrochemical Society, 1978, p 479
13. M.J. Streicher, *Corrosion*, Vol 30, 1974, p 77
14. W. Yang, R. Chang, H.-Z. Hua, *Corros. Sci.*, Vol 24, 1984, p 691
15. V. Mitrovic-Scepanovic and M.B. Ives, *J. Electrochem. Soc.*, Vol 127 (No. 9), 1980, p 1903
16. D.C. Agarwal and U. Heubner, *Proc. 12th Int. Corrosion Congress*, NACE International, Vol 3A, 1993, p 1226
17. Y.C. Lu and C.R. Clayton, *J. Electrochem. Soc.*, Vol 132, 1985, p 251
18. Y.C. Lu, C.R. Clayton, and A.R. Brooks, *Corros. Sci.*, Vol 29, 1989, p 863
19. Y.C. Lu, M.B. Ives, and C.R. Clayton, *Corros. Sci.*, Vol 35 (No. 1-4), 1993, p 89
20. K. Hasimoto, K. Asami, and K. Teramoto, *Corros. Sci.*, Vol 19, 1979, p 3
21. M. Sivakumar, U. Kamachi Mudali, and S. Rajeswari, *Steel Res.*, Vol 65 (No. 2), 1994, p 79
22. M. Sivakumar, U. Kamachi Mudali, and S. Rajeswari, *J. Mater. Sci. Lett.*, Vol 13, 1993, p 142
23. J. Kruger, *Int. Mater. Rev.*, Vol 33 (No. 3), 1988, p 142
24. T.P. Hoar and W.R. Jacob, *Nature*, Vol 216, 1967, p 1299
25. B. MacDougall and M. Cohen, *J. Electrochem. Soc.*, Vol 121 (No. 9), 1974, p 1152